AIP | Review of Scientific Instruments

Measurement of dynamic polarization modulation depth utilizing the J 1–J 4 method of spectrum analysis

V. S. Sudarshanam and S. B. Desu

Citation: Review of Scientific Instruments **65**, 2337 (1994); doi: 10.1063/1.1144685
View online: http://dx.doi.org/10.1063/1.1144685
View Table of Contents: http://scitation.aip.org/content/aip/journal/rsi/65/7?ver=pdfcov
Published by the AIP Publishing

Measurement of dynamic polarization modulation depth utilizing the J_1–J_4 method of spectrum analysis

V. S. Sudarshanam and S. B. Desu
Department of Materials Science and Engineering, Virginia Polytechnic Institute and State University, Blacksburg, Virginia 24061-0237

(Received 6 December 1993; accepted for publication 16 April 1994)

A spectrum analysis method for the linear, direct, and self-consistent measurement of dynamic modulation depth of polarization modulators is presented. This method utilizes the Bessel recurrence relation to determine the modulation depth from the photodetector voltage amplitudes at the fundamental frequency and its next three harmonics. Based on the existing J_1–J_4 method of dynamic phase-shift measurement in homodyne interferometry, this method is useful for calibration of polarization modulated ellipsometers. The method is demonstrated through the use of a highly birefringent transparent thin film of piezoelectric polyvinylidene fluoride with indium tin oxide electrodes. The theoretical analysis of the measured noise factor for the particular system configuration predicted a minimum detectable polarization modulation depth of 0.2 rad, and was experimentally verified.

I. INTRODUCTION

Polarization modulation ellipsometry (PME) has been established[1–4] as a direct and sensitive technique for the optical characterization of materials in several applications related to growth and etching processes, and surface analysis, of semiconductor thin films, antireflection coatings, ceramics, and other materials. In comparison to other ellipsometric techniques, such as the nulling and the rotating analyzer (or the rotating polarizer) kinds, the PME technique offers certain advantages, such as high speed with no mechanically rotating optical components, that are particularly useful for real-time *in situ* intelligent processing of materials. Whereas the precision of the PME and the rotating analyzer ellipsometer (RAE) is comparable, the PME involves greater complexity and could lead to lower accuracy in comparison to RAE, due to the nonideal behavior of the polarization modulator.[2] The PME commonly utilizes a birefringent photoelastic modulator that generates at a frequency of 50 kHz a sinusoidal relative retardation between the orthogonal electric-field components transmitted through it. The measured ellipsometric parameters,[1–5] Δ and Ψ, are utilized to derive the refractive index n and the extinction coefficient k of the optical system of interest. These ellipsometric parameters are measured in such a configuration from the photovoltage monitored at the fundamental frequency and the second harmonic, normalized with respect to the dc component under the significant condition that the input voltage applied to the modulator generates a dynamic polarization modulation depth m of exactly 2.405 rad for which the value of the Bessel function of the first kind and zeroth order, $J_0(m)$, is equal to zero. Such a condition[1–4] results in a relatively simple and straightforward relationship between the photovoltage amplitudes and the parameters Δ and Ψ. However, for achieving a precision of the order of 0.001° for these measured ellipsometric parameters, it can be shown, as done in the next section, that the modulator must be driven such that the deviation from the optimum point of $m=2.405$ rad is minimum. This necessitates that the response of the modulator to the applied input voltage be precisely known and controlled in the presence of ambient fluctuations. Indeed, for the purposes of spectroscopic ellipsometry,[1,2] the dependence of the retardation on the wavelength requires that the drive voltage be increased linearly with the wavelength to fulfill the condition for optimum m, within the assumption that the dispersion of the modulator birefringence is negligible. Such a requirement will be fulfilled only if the relationship between the applied input voltage and the response of the modulator is linear. On the other hand, a recent report[5] of the PME technique modified for application to the measurement of ultralow birefringence in single mode optical fibers utilized an arbitrary value for m. In both of these cases, there exists a strong need for the characterization of the modulator in terms of the linearity of response and the frequency response.

The direct calibration of dynamic phase shift by the J_0(null) method,[6] and there from the determination of the frequency response and the phase shifting coefficient of modulators, was demonstrated earlier for optical interferometers. This method was based on the visual observation of the disappearance of the spatial fringe pattern when the zeros of $J_0(m)$ are crossed. However, this fast and direct calibration technique could not be utilized here for polarization modulation because the optical arrangement was not configured to form any spatial fringe pattern. Such characterization[7] of the modulator for polarization modulation has been performed commonly by methods such as the J_3/J_1 technique. This J_3/J_1 technique utilizes the ratio of the photovoltage amplitudes at the third harmonic and the fundamental frequency to measure the value of m. However, this requires an inversion of the Bessel function ratio to arrive at the value for m. In contrast, a linear, self-consistent and direct readout of the dynamic phase shift in a fiber-optic homodyne interferometer without the need for any feedback, source stabilization, or visibility control was demonstrated recently through the J_1–J_4 technique.[8,9] The voltage amplitudes at the fundamental frequency and its next three harmonics were determined from a fast Fourier transform of the photodetector output and

 0034-6748/94/65(7)/2337/7/$6.00

substituted in the Bessel recurrence relation to determine the dynamic phase modulation depth [see, for instance, Eq. (11)]. The minimum detectable phase shift was 0.1 rad, with the error for a given phase shift being shown[10] to be dependent on the noise factor K arising from the low-frequency $1/f$ noise of the several components forming the system. This paper presents experimental results of the linear, direct, and self-consistent measurement of the dynamic polarization modulation depth through the use of the J_1–J_4 spectrum analysis technique hitherto used only for interferometry. Further, in contrast to the photoelastic modulators utilized in earlier reports, a freestanding, highly birefringent, thin, optically transparent, piezoelectric polyvinylidene fluoride (PVDF) film of thickness ~64 μm is used as a test element for the generation of polarization modulation in a typical bulk optic transmission ellipsometric arrangement. The electrodes on the PVDF film are made of indium tin oxide (ITO) which is transparent for the wavelengths of interest here. It is known[5] that the photoelastic modulator element utilized in the earlier configurations vibrates on rubber mounts causing the light beam to wander, necessitating the positioning of the optical fiber under test before the modulator to avoid fluctuations in the fiber launch efficiency. The use of a relatively thin film in this work eliminates such problems and can be (a) directly bonded onto, or (b) simply butt-coupled or juxtaposed to the fiber endface at the input end or at the output end. This fiber-PVDF configuration was demonstrated recently[11] to perform reliably for generating dynamic phase modulation in an extrinsic fiber-optic Fabry–Perot interferometric (FPI) configuration combined concurrently with a hybrid Mach Zehnder interferometric configuration.

The specific freely supported configuration of the ITO-electroded PVDF film (polarization) modulator utilized in the work presented in this paper will hereafter be referred to as the IPM. The need for the modulator characterization is emphasized in Sec. II, based on the error in the measurement of the ellipsometric parameters as a function of the deviation of the modulation depth from the optimum value. The experimental arrangement and the detection scheme used for the measurement of polarization modulation in the IPM are described in Sec. III. The experimental results for the linearity of response and frequency response of the IPM along with the determination of the noise factor are presented and discussed in Sec. IV, followed by the conclusion.

II. NEED FOR MODULATOR CHARACTERIZATION

A serial arrangement of the laser source, the linear polarizer (P), the modulator (M), the sample (S) to be tested, and the analyzer (A), the principal axes of each at 45° to the adjacent element (see Fig. 1 of Ref. 4), is considered for the purposes of the analysis in this section. It is assumed that the electric field of the incident light is of unit amplitude, and that the optical components are perfect. The orientations of P, M, and A are 90°, +45°, and −45°, with all the azimuths measured from the direction (perpendicular to the plane of incidence) of the linear eigenpolarization of the sample S. The intensity seen at the detector for this particular arrangement is given by[1,3,4]

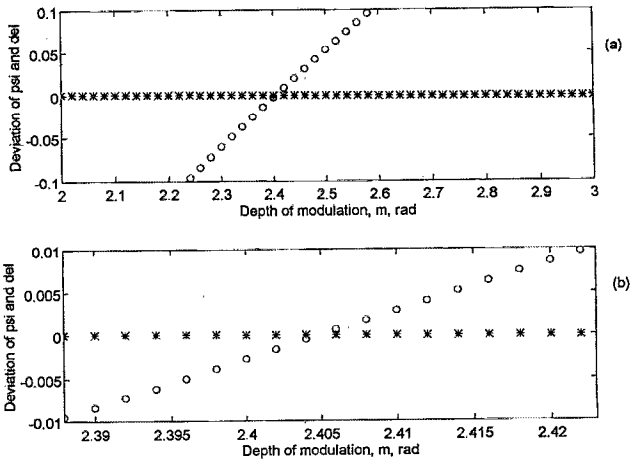

FIG. 1. The deviations $\delta\Psi$ (asterisks) and $\delta\Delta$ (open circles) of the measured values Ψ' and Δ' from the ideal values Ψ and Δ as a function of the value of the depth m of polarization modulation around the optimum value of 2.405 rad. The plots (a) and (b) show different ranges of the vertical and horizontal axes. Values of $N=0.014$ and $S=0.8055$ were assumed.

$$I=(1/4)(r_s^2+r_p^2)[1+\sin(2\Psi)\sin(\Delta)\sin(\phi) + \cos(2\Psi)\cos(\phi)], \quad (1)$$

where the well-known[1,3] standard substitutions of $\tan(\Psi)=r_p/r_s$ and $\Delta=\delta_p-\delta_s$ have been made, and $\phi=m\sin\omega t$, where m is the depth of polarization modulation generated by the modulator at the angular frequency of ω. Expanding[8,9] Eq. (1) in terms of the Bessel functions J_n of the first kind and order n, and considering only the fundamental frequency and second-harmonic components, I_f and I_{2f}, respectively, of the intensity variation expressed by Eq. (1), one has, under the significant assumption that the condition $J_0(m)=0$ (or $m=2.405$ rad) is fulfilled,

$$R_1=I_f/I_{dc}=\sin(2\Psi)\sin(\Delta)[2J_1(m)], \quad (2)$$

$$R_2=I_{2f}/I_{dc}=\cos(2\Psi)[2J_2(m)], \quad (3)$$

where $I_{dc}=(1/4)(r_s^2+r_p^2)$ when $m=2.405$ rad; R_1 and R_2 are normalized amplitudes at the fundamental and second-harmonic frequencies that can be calibrated to form the quantities $R_{c1}=[2J_1(m)]$ and $R_{c2}=[2J_2(m)]$ by using, respectively, a circular analyzer and a linear analyzer in between the modulator and the sample.[1,3] The ellipsometric parameters Δ and Ψ are thus obtained from the equations

$$R_1/R_{c1}=\sin(2\Psi)\sin(\Delta)=(1-N^2)^{1/2}\sin(\Delta), \quad (4)$$

$$R_2/R_{c2}=\cos(2\Psi)=N. \quad (5)$$

The value of N (which provides the value of Ψ) is first obtained from Eq. (5) and then substituted into Eq. (4) to obtain the value of Δ.

We now consider the effect of a deviation of the value of m from the optimum value of 2.405 rad. On taking into account the dc contribution to the intensity from the $J_0(m)$ component, the deviation of the measured values Ψ' and Δ' from the ideal values of Δ and Ψ as given by Eqs. (2)–(5) can be obtained from

$$\Psi' = (1/2)\cos^{-1}([1-\tan^2(\Psi)]/\{[1+\tan^2(\Psi)] + [1-\tan^2(\Psi)]J_0(m)\}), \quad (6)$$

$$\Delta' = \sin^{-1}[2\tan(\Psi)\sin(\Delta)/(\sin(2\Psi')\{[1+\tan^2(\Psi)] + [1-\tan^2(\Psi)]J_0(m)\})]. \quad (7)$$

Figure 1 shows the deviation of the measured values Δ' and Ψ' from the ideal values Δ and Ψ, respectively, as a function of the value of m. For the purposes of Fig. 1, the values of $N=0.014$ and $S=0.8055$, where $S=\sin(\Delta)$, were assumed from the data reported in Ref. 1 for the deposition of a 1000 Å thick Ag. It can be seen from the two plots shown in Fig. 1 that the deviation of Ψ is less than 0.001° for values of m between 2.1 and 2.8 rad, for the chosen values of N and S. However, the deviation of Δ is less than 0.01° only for values of m between 2.388 and 2.422 rad. Equations (6) and (7) can also be rewritten as follows in order to see the dependence of the errors $d\Psi$ and $d\Delta$ on the ideal values Ψ and Δ:

$$d\Psi = -(N^2 J_1(m)/\{2(1-N^2)^{1/2}[1+NJ_0(m)]^2\})dm, \quad (8)$$

$$d\Delta = \{(\tan\Delta)NJ_1(m)/[1+NJ_0(m)]^2\}dm. \quad (9)$$

The Bessel function identity $\{d[J_0(m)]/dm = -J_1(m)\}$ was utilized in arriving at the expressions in Eqs. (8) and (9). To determine the error when the value of m deviates from the optimum value of 2.405 rad, the values of $J_0(m)=0$ and $J_1(m)\sim 0.52$ can be substituted in Eqs. (8) and (9). Thus, it can be seen that the error $d\Delta$ can be very large even for a small dm if $\tan\Delta$ becomes very large. Alternatively, as described in Ref. 12, one can perform two successive scans over the same wavelength range to measure either the pair (N,S) or the pair (N,C), where $C=\cos\Delta$. The choice of the more accurate pair would be decided by whether S or C is smaller. These considerations show that there exists a stringent need for control of the value of m within limits determined by the desired accuracy of measurement of Δ and Ψ. In practice, it is the voltage that is applied to the modulator that would be controlled to derive the desired value of m. As mentioned in Sec. I, under the assumption that the dispersion of the induced birefringence is negligible, spectroscopic studies using the PME technique require the linear increase of the input voltage with the wavelength. The modulation amplitude is assumed to be effectively a function only of the ratio (V/λ), V being the peak voltage applied to the modulator and λ, the wavelength of light. The determination of the linearity of response with input voltage at one chosen wavelength would lead to the determination of the linearity of the required input voltage as a function of the wavelength to keep the value of m at the optimum value. This linearity of response with the input voltage can be determined with the use of the direct reading J_1–J_4 technique hitherto used for linear measurements of phase shift alone in interferometers.

Moreover, an inspection of the Eqs. (1)–(3) would show that any static birefringence that is not canceled effectively would result in a cross modulation[5] of the original terms R_1 and R_2 measured at the fundamental and second-harmonic frequencies. This can be seen by expressing the quantity ϕ in Eq. (1) as $\phi = m\sin(\omega t) + \phi_d$, where ϕ_d is the static retardation. The effect of this static retardation can be significant when ultralow birefringence fibers are being tested. This problem assumes importance for modulator materials that exhibit a temperature dependence[7] of the static birefringence. As the ambient temperature fluctuates, the modulator would thus lead to inaccurate measurements of the ellipsometric parameters. The temperature can be controlled in crystal modulators of the kind investigated in Ref. 7. However, piezoelectric thin films made of PVDF are also pyrolectric and sensitive to temperature, thus making uniform control of the temperature over an appreciable area in a longitudinal modulator configuration as utilized here or in Ref. 11 very difficult. Thus there exists a need for characterizing the variation of ϕ_d with temperature. The earlier reports[8,13,14] of both the flat strip and coiled fiber-on-PVDF film (FPF) modulators have shown that the frequency response of the PVDF modulators exhibits strong resonance peaks. It has also been shown in the reports for those configurations that the response with respect to the input voltage becomes increasingly nonlinear near the resonance peaks. Thus, it would be desirable to determine the frequency response of the IPM and quantify the linearity of response with the input voltage at chosen frequencies, and to operate the IPM at a frequency where a large polarization modulation depth can be obtained retaining the linear behavior. The experimental arrangement and the detection scheme utilized for characterizing the IPM are described in the next section.

III. EXPERIMENTAL ARRANGEMENT AND SIGNAL DETECTION

The geometry and structural arrangement of the IPM element is described first, followed by the experimental arrangement and technique for the measurement of the dynamic polarization modulation. In the preliminary tests of the device performance of the IPM, the piezofilm with the transparent ITO electrodes was clamped, by the use of an epoxy, between two identical circular metal washers of inner diameter 6 mm and outer diameter 1 cm. This epoxied piezofilm-washer structure was then attached to a rubber ring mounted on a rotary stage. The wire leads providing the electrical input were soldered to copper foil strips in contact with the piezofilm directly by using an adhesive tape or by using a conducting silver-loaded epoxy. The preliminary results of polarization modulation for this circularly clamped configuration, as reported in detail in Ref. 11, can be summarized as follows: (a) a strong resonance peak for this circularly clamped configuration was observed at 8.4 kHz, (b) a highly linear response of the intensity modulation amplitude arising from polarization modulation was observed at the resonance frequency of 8.4 kHz, and (c) it was verified by inserting and subsequently removing an analyzer that the intensity modulation indeed was the result of the polarization modulation and not any other competing reflection related interference effects. Though the intensity modulation was highly linear with the input voltage, the depth of polarization modulation, denoted by m, generated by the circularly clamped configuration was not large enough to be determined by the conventional methods of spectrum analysis. The value of m can be

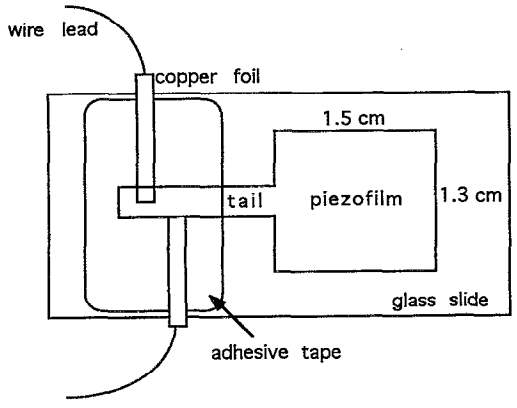

FIG. 2. Geometry and structural arrangement for the freely supported IPM element.

determined[8] from the photovoltage amplitude at the fundamental frequency V_1 only if the instantaneous values of the intensity incident on the detector, the drift in static retardation due to ambient fluctuations, and the visibility are known accurately. This would also require knowledge of the transmittance of the individual optical components used in the setup. However, in the presence of more than one peak in the frequency spectrum of the detector output, methods[8] utilizing the ratios such as (V_3/V_1), where V_i is the voltage amplitude at the ith frequency, can be implemented to measure indirectly the value of m. Such measurements require inversion of the Bessel function ratios and are not desirable in actual practice. The use of the linear and direct reading J_1–J_4 technique requires the generation of greater than 0.1 rad of phase modulation depth for a typical interferometric configuration.[8] In other words, the amplitudes at the fundamental and its next three harmonics should be higher than the noise floor at their respective frequencies. To achieve a polarization modulation depth that would be appreciable enough, a freely supported configuration of the IPM was tested. It should be noted that the freely supported configuration was utilized solely for the purpose of demonstration of the measurement technique. Practical considerations of device design in coupling optical fibers to the piezofilm may require at least partial constrainment for stability. A rectangular piece of the piezofilm, of thickness 63.9 μm and areal dimensions shown in Fig. 2, with a tail of small width extending in one direction was freely supported on a glass slide of thickness 1 mm. The tail portion of the film was attached to the slide by an adhesive tape while the major rectangular portion of the film was pressed against the slide by the slight natural convex curvature of the film. The slight natural curvature thus provided a stable positioning of the film without causing any loading effects as in the earlier epoxied circularly clamped configuration. The intensity modulation produced on the application of the electrical signal was verified for its origin in polarization modulation by using an analyzer, as described earlier in Ref. 11.

The experimental arrangement used for the characterization of the linearity of response and the frequency response of the IPM is shown in Fig. 3. The optical transmittance of the PVDF piezofilm along with the ITO electrodes measured

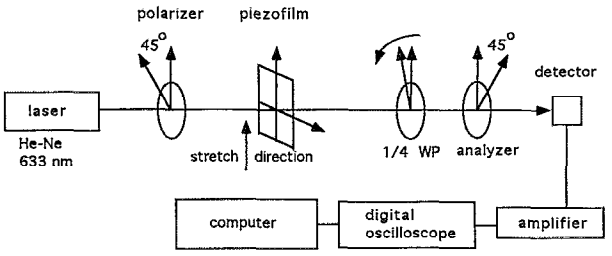

FIG. 3. Experimental optical arrangement for the study of polarization modulation generated by the IPM. WP stands for wave plate.

as a function of the wavelength using an UV-VIS-NIR scanning spectrophotometer, showed a value of ~71.7% at 633 nm, and of ~89% at the higher wavelength regions around ~1300 nm. However, for convenience, the light from a He-Ne laser operating at 633 nm was used. The polarizer in Fig. 3 was aligned at an angle of 45° to the stretch direction of the piezofilm. The piezofilm, as obtained from the manufacturer, would show macroscopic straight lines on the surface which can be seen by visual inspection. The intrinsic birefringence of the piezofilm, measured for the sample used here to be 0.0328 between the directions along and perpendicular to the stretch axis, arises mainly from the polar orientation of the molecules along the direction of the applied uniaxial stretch necessary to make the polymer film piezoelectric.[15] Thus, the eigenaxes of polarization for the piezofilm would naturally be along and perpendicular to the stretch direction. In practice, a laser beam of small dimensions would generate a band of scattered light in both the forward and backward directions as it traverses the piezofilm. This band of light would be perpendicular to the stretch direction and can be utilized to estimate relative angles directly. The analyzer was crossed with respect to the polarizer. A quarter-wave plate was included in this serial arrangement to achieve linear intensity modulation. The quarter-wave plate was adjusted[7] for 50% transmission in the absence of the applied voltage.

The output of the photodetector was amplified and fed into a digital oscilloscope. The time domain signal from the oscilloscope was transferred to a computer which performed a fast Fourier transform (FFT) to provide a frequency spectrum of the detector output. The instantaneous voltage at the output of the detector assembly can be written as

$$V=(V_0/2)\Bigg[1-\cos\Delta\phi_R\Bigg(J_0(m)+2\sum_{n=1}^{\infty}J_{2n}(m)\cos(2n\omega t)\Bigg)+\sin\Delta\phi_R\Bigg(2\sum_{n=1}^{\infty}J_{2n-1}(m)\sin[(2n-1)\omega t]\Bigg)\Bigg], \tag{10}$$

where V_0 is the photovoltage due to the average intensity of the light incident on the detector, the J_n's are the Bessel functions of the first kind and order n, m is the depth of

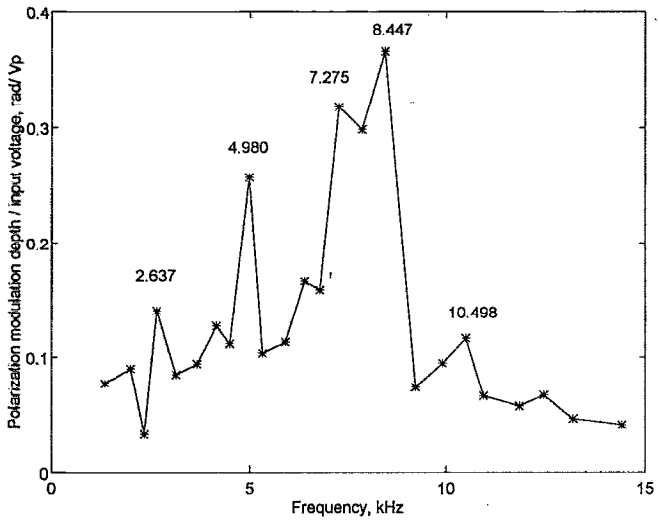

FIG. 4. Frequency response of the IPM in terms of the ratio of the depth m measured by the J_1–J_4 technique, to the input voltage as a function of the signal frequency.

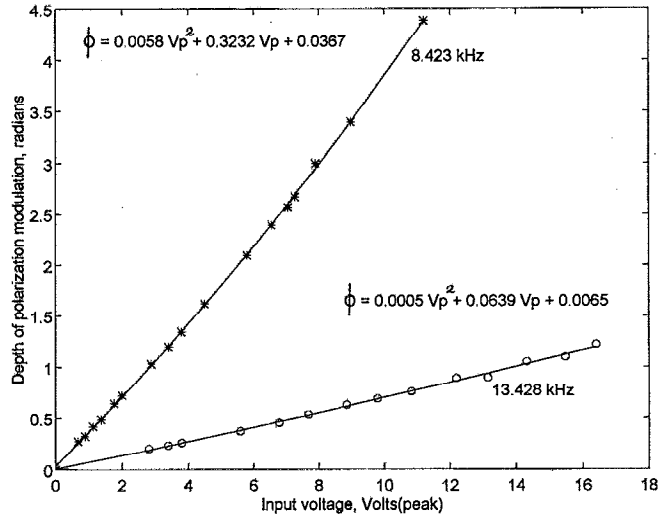

FIG. 5. The depth m measured by the J_1–J_4 technique as a function of the input voltage applied to the IPM at frequencies (a) 8.423 kHz (asterisks) and (b) 13.428 kHz (open circles). The least-squares fit to these plots is also shown.

polarization modulation, and ω is the angular frequency of the signal. The phase term due to static birefringence of the piezofilm has been lumped with the phase terms due to the quarter-wave plate and the random drifts to form a total phase term $\Delta\phi_R$ in Eq. (10). It must be pointed out that although Eq. (10) bears a close resemblance to the expression for the instantaneous intensity in an interferometer, the intensity modulation can be observed only if polarization sensitive elements are present. It must be noted (a) that the sample in the arrangement corresponding to Eq. (1) is nonexistent in the arrangement of Fig. 3 as it is the modulator itself that is being characterized here and not the sample, and (b) that the instantaneous value of the term $\Delta\phi_R$ in Eq. (10) is relatively irrelevant to the measurement of m which is, in fact, the unique feature of the J_1–J_4 technique. The J_1–J_4 technique utilizes the Bessel recurrence relation for measuring m directly, irrespective of random drifts in the polarization state due to ambient fluctuations, source intensity fluctuations, and changes in visibility; thus[8]

$$m^2 = 24V_2V_3/(V_1+V_3)(V_2+V_4), \tag{11}$$

where V_i is the amplitude of the photovoltage, expressed by Eq. (10), at the ith frequency.

IV. RESULTS AND DISCUSSION

The frequency response of the IPM utilizing the freely supported piezofilm is shown in Fig. 4 in terms of the ratio of the depth of polarization modulation m as measured through the expression in Eq. (11), to the value of the applied voltage. This normalization with respect to the input voltage was done because the value of m varied by a large amount between the resonance frequencies and others, necessitating the lowering of input voltage at the resonance frequencies to keep the value of m within the linear range of measurement. As shown later [see Fig. 7(a)], this linear range extends from the minimum detectable polarization depth, m(min), to nearly the value of m (~5.1 rad) at which the first zero for the Bessel function J_2 occurs. Also, as the first zero of the Bessel function J_1 is crossed at $m=3.83$ rad, the sign of the voltage V_1 in Eq. (11) should be changed from positive to negative for $m>3.83$ rad. Whereas this change in sign is easily done in the calculation of m by the computer, the measurement of m would be erroneous at the points where either J_2 or J_3 become zero, or where $J_1=-J_3$, or $J_2=-J_4$. It is important to study the behavior of Eq. (11) to avoid serious errors in the characterization of the modulator's frequency response when the range of m generated has not been estimated. A qualitative study of the frequency response with observation of the relative magnitude of the peaks in the displayed FFT helps overcome such errors. The frequency response as shown in Fig. 4 for the freely supported IPM exhibits a significant peak at 8.447 kHz with appreciable peaks seen at other frequencies of 4.98 and 7.275 kHz. Comparing this with the most significant resonance peak at 8.4 kHz in the frequency response obtained for the circularly clamped modulator in Ref. 11, it can be seen that clamping the piezofilm circularly results in a selective enhancement of the response at the resonance frequency of 8.4 kHz and its harmonic at ~16.6 kHz, and relative suppression of the peaks at other frequencies.

The linearity of response of the IPM was tested, by using the J_1–J_4 technique, at the two frequencies of 8.423 and 13.428 kHz. The value of m measured as a function of the input voltage is shown in Fig. 5 for these two frequencies. In agreement with the frequency response plotted in Fig. 4, the linear coefficient of polarization modulation, namely 0.064 rad/Vp at the nonresonance frequency of 13.428 kHz is much less than that of 0.323 rad/Vp at the resonance frequency of 8.423 kHz. In contrast to the FPF modulators,[13,14] the response of the IPM was largely linear even at the resonance frequency. This difference is attributed to the appreciable amount of epoxy commonly used in the FPF configuration.

The value of m for low values of the input voltage below

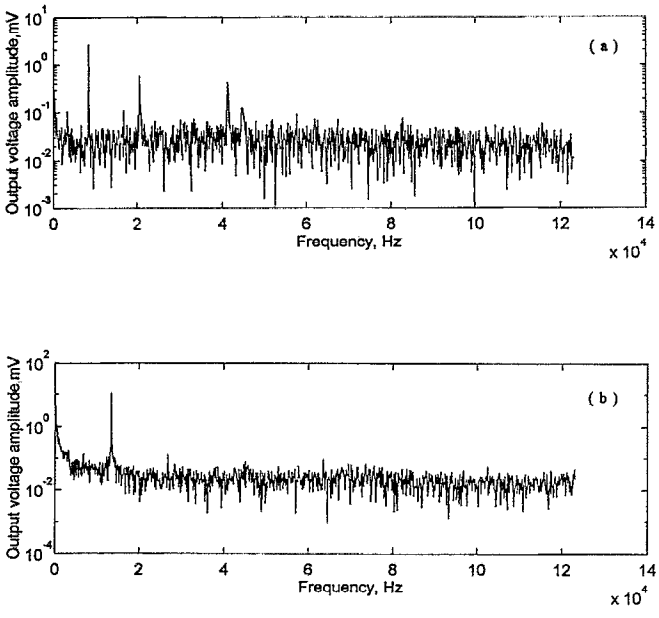

FIG. 6. FFT of the photovoltage for an input voltage of (a) 1.373 Vp at 8.423 kHz and (b) 3.403 Vp at 13.428 kHz. Note that the vertical axes have a logarithmic scale.

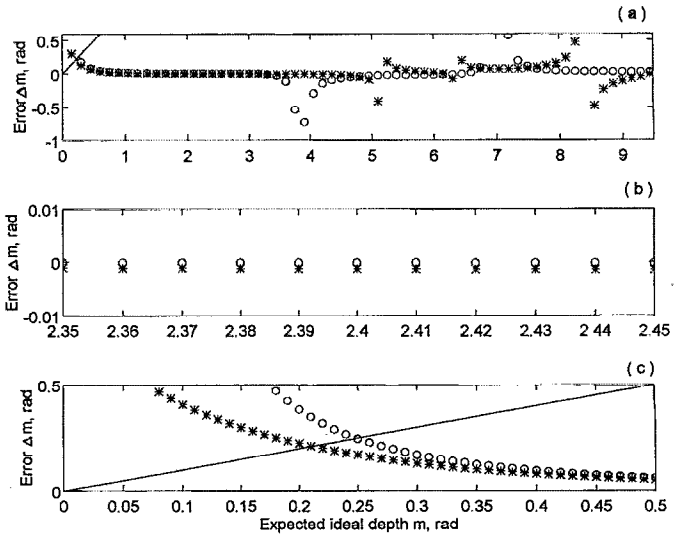

FIG. 7. The error Δm between the measured value m' and the ideal value m as a function of the value of m for the J_1–J_4 technique (asterisks) and the J_3/J_1 technique (open circles), shown over three different ranges of the vertical and horizontal axes. The straight line ($m=m$) is also shown in (c).

~0.67 Vp at 8.423 kHz and ~2.81 Vp at 13.428 kHz showed an increase with decreasing values of the input voltage. Such a behavior was expected in similarity to measurements of the dynamic phase shift in the interferometric applications.[8,10] The minimum detectable polarization depth, m (min) and the accuracy of measurement of m, can be determined through the noise analysis developed in Ref. 10 earlier for the interferometric case. Figures 6(a) and 6(b) show the frequency spectrum of the photovoltage as provided by the FFT for an input voltage of 1.373 Vp at 8.423 kHz, corresponding to m of 0.544 rad, and of 3.403 Vp at 13.428 kHz, corresponding to m of 0.234 rad. On taking the ratio of the voltage amplitude V_1 of the peak at the fundamental frequency and that of the noise floor ΔV_1, seen at that frequency in each of the two plots in Fig. 6, and substituting their values in the expression $K=(\Delta V_1/V_1)[J_1(m)]$, the value obtained for K at 8.423 kHz was 0.002, while that at 13.428 kHz was 0.0007. This difference in the values of K for the same optical system was due to the setting of the amplifier for measurements at 13.428 kHz to a higher gain by a factor of about ten compared to that at 8.423 kHz. This can be seen from the vertical scale range for the two plots, and the fact that the value of $J_1(m)$ is proportional to m for such low values of m.

With the measured value of the noise factor K of 0.002 at the frequency of 8.423 kHz, the value of m(min), and the error Δm was determined through the following theoretical expression for the experimentally measured value m' in relation to the expected ideal value of m:

$$(m')^2=24[J_2(m)+K/2][J_3(m)+K/3]/(J_1(m)+J_3(m)+1.33K][J_2(m)+J_4(m)+0.75K]. \tag{12}$$

Figure 7 shows three plots of the variation of the error Δm as a function of the ideal value of m for three different ranges of the horizontal and vertical axes. Also included for comparison in the same figure are similar plots for the J_3/J_1 method. The expression for the error with the use of the J_3/J_1 method becomes complicated because the value of m has to be obtained through inversion and not through the exact mathematical identity of the Bessel recurrence relation. The expression for the ratio J_3/J_1 considering the first two terms in the general power-series expansion[16] for $J_n(m)$ can be written as

$$[J_3(m)/J_1(m)]=(16m^2-m^4)/[16\times(24-3m^2)]. \tag{13}$$

It should be noted that the simple expression of $(J_3/J_L)=(m^2/24)$, obtained when only the first term in the power-series expansion is considered, does not hold good for appreciable values of m. The error Δm in the measurement through the J_3/J_1 method is then given by

$$\Delta m=\{[(J_3+K/3)/(J_1+K)]-(J_3/J_1)\}/R, \tag{14}$$

where R stands for the expression for the derivative of the ratio on the right-hand side of Eq. (13). As can be seen from Fig. 7(a), the range of measurement for the J_3/J_1 method breaks first at the value of $m=3.83$ rad where the first zero of $J_1(m)$ occurs, whereas the range for the J_1–J_4 technique breaks first at the value of $m=5.1$ rad where the first zero of $J_2(m)$ occurs. A simple calculation based on linear relations would show that the voltage needed at 2000 nm for the IPM at 8.423 kHz to provide a value of 2.405 rad for m would correspond to the voltage of about 20.66 Vp when 633 nm is used. This voltage of 20.66 Vp would generate a depth of 9.2 rad at 633 nm according to the least-squares fit shown in Fig. 5. Thus, as seen from the plot in Fig. 7(a), the J_1–J_4 and the J_3/J_1 techniques can be used complementarily to determine the linearity in the higher ranges of modulation depth. However, if the wavelength is varied when the characterization is being performed, the value of m measured can be kept

closely around 2.405 rad. In such a case, the errors in measurement for the particular value of K of 0.002 is very close for both the methods as shown in Fig. 7(b). On the other hand, for example, if in the characterization process the voltage at 2000 nm is maintained the same as for providing 2.405 rad at 633 nm, the depth m generated at 2000 nm would be ~0.316 rad. To investigate the error in the measurement of m for such low values, the region of lower m in Fig. 7(a) is shown enlarged in Fig. 7(c). The minimum detectable depth, $m(\min)$ occurs at the point where the straight line ($m=m$) meets the curve for the error Δm. Thus, as seen from Fig. 7(c), the value $m(\min)$ for the J_1–J_4 and the J_3/J_1 techniques are 0.21 and 0.25 rad, respectively, for the value of K of 0.002. The value of $m(\min)$ as obtained from the theoretical noise analysis for the J_1–J_4 technique agreed closely with the corresponding experimental voltages below which the measured m increased with decreasing voltage for the two frequencies of 8.423 and 13.428 kHz considered. The value of $m(\min)$ can be kept suitably lower from the value of m(~0.316 rad for 2000 nm) generated at the largest wavelength of interest by lowering the value of K.

The J_1–J_4 technique hitherto utilized only for phase-shift measurements in interferometry was demonstrated to provide a linear and direct readout of the dynamic polarization modulation depth for use in ellipsometric applications. Based on theoretical expressions for the error in measurement of the ellipsometric parameters, the need for the characterization of the polarization modulator in terms of the linearity of response and frequency response was brought out. The polarization modulator consisting of a PVDF piezofilm with transparent ITO electrodes and freely supported on a glass slide was characterized for performance. A linear coefficient of polarization modulation of 0.323 rad/Vp at the resonance frequency of 8.423 kHz and of 0.064 rad/Vp at the nonresonance frequency of 13.428 kHz were measured by the J_1–J_4 technique. The theoretical and experimental values for the minimum detectable depth for the particular configuration utilized agreed closely for both the frequencies.

ACKNOWLEDGMENTS

This work was partially supported by the Advanced Research Projects Agency through the Office of Naval Research. V.S.S. thanks David Port of Atochem Sensors, Inc. for providing the piezofilm, and John Jackson of Metricon Corp. for measurements of the piezofilm indices and thickness.

[1] S. N. Jasperson, D. K. Burge, and R. C. O'Handley, Surf. Sci. **37**, 548 (1973).
[2] R. W. Collins and K. Vedam, in *Encyclopedia of Applied Physics* (VCH, New York, 1993), Vol. 6, p. 201.
[3] R. M. A. Azzam and N. M. Bashara, *Ellipsometry and Polarized Light* (North-Holland, Amsterdam, 1977).
[4] R. C. O'Handley, J. Opt. Soc. Am. **63**, 523 (1973).
[5] A. J. Barlow, J. Lightwave Technol. **LT-3**, 135 (1985).
[6] V. S. Sudarshanam and K. Srinivasan, Opt. Lett. **14**, 1267 (1989).
[7] R. T. Denton, F. S. Chen, and A. A. Ballman, J. Appl. Phys. **38**, 1611 (1967).
[8] V. S. Sudarshanam and K. Srinivasan, Opt. Lett. **14**, 140 (1989).
[9] W. Jin, L. M. Zhang, D. Uttamchandani, and B. Culshaw, Appl. Opt. **30**, 4496 (1991).
[10] V. S. Sudarshanam, Appl. Opt. **31**, 5997 (1992).
[11] V. S. Sudarshanam, S. B. Desu, and R. O. Claus, Proc. Mater. Res. Soc. (in press).
[12] S. N. Jasperson and S. E. Schnatterly, Rev. Sci. Instrum. **40**, 761 (1969).
[13] V. S. Sudarshanam and K. Srinivasan, J. Appl. Phys. **68**, 1975 (1990).
[14] V. S. Sudarshanam and R. O. Claus, J. Lightwave Technol. **11**, 595 (1993).
[15] D. K. Das-Gupta, K. Doughty, and D. B. Shier, J. Electrostat. **7**, 267 (1979).
[16] See, for example, G. Arfken, *Mathematical Methods for Physicists*, 3rd ed. (Academic, New York, 1985).